Proceedings of the Canadian Society for Mechanical Engineering International Congress 2022
CSME Congress 2022
June 5-8, 2022, Edmonton, AB, Canada

Capture and thermal inactivation of airborne Covid-19 particles

Reza Zarghanishiraz[1], Mojtaba Zabihi[1], Ri Li[1*], Jonathan Little[2], Vicki Komisar[1]
[1]School of Mechanical Engineering, University of British Columbia, Kelowna, Canada
[2]School of Health and Exercise Sciences, Faculty of Health and Social Development, University of British Columbia, Kelowna, Canada
*Sunny.li@ubc.ca

Abstract— For centuries, people have been fighting airborne transmitting diseases like the common cold virus, influenza or Measles and Tuberculosis as examples of more fatal diseases. Certainly, one of the most catastrophic viruses among the airborne transmitting diseases is Covid-19 which has taken millions of lives in the past three years. Although vaccines have significantly diminished the rate of deaths, periodic emergence of different variants like Delta and Omicron proves that vaccination is not a substitution for the virus-spread controlling methods. Subsequently, it is still necessary to prevent the spread of the virus from the very beginning by using masks and sterilizing the air in indoor spaces. In the present work, a novel method for both trapping and inactivation of the airborne transmitting pathogens is provided. Contaminated air passes through multiple layers of fine woven meshes while the mesh is acting as both a filter to remove the airborne particles and also as a heating element to raise the air temperature. $D_{50} = 0.9\ \mu m$ which means that 50%-removal efficiency occurs for $0.9\ \mu m$ particles in this device. According to the exponential relationship of the temperature and the exposure time models, taking the air to high temperatures like 150°C provides 3-log virus load reduction (i.e. 99.9% inactivation of the viruses) in a fraction of a second. Numerical simulations are conducted using ANSYS Fluent software and experimental tests are in progress to validate the numerical data.

Keywords-component; airborne disease, thermal inactivation, particle tracking, particle trap, air sterilization

I. INTRODUCTION

According to the World Health Organization (WHO), more than 5.5 million people have died from the Covid-19 virus worldwide and more than 300 million people got infected with this virus up to the date of this publication [1]. Coronavirus is known as an airborne-transmitting disease and can be spread through particles and aerosols as a result of cough, sneeze, or regular talking of an infected person [2-4]. Nose or mouth contact after touching contaminated surfaces is another way of virus transmission. Although vaccines have diminished the spread rate of the virus significantly globally and the death rates have notably decreased [5], the emergence of the highly contagious Omicron variant has proved that further actions are required for fighting this disease. One of the challenges regarding vaccination is their temporary effect that requires people to recover their immunity against the virus by periodic injections as some countries are getting ready for the fourth dose of their vaccines[6].

Furthermore, looking back through the history of humankind, Covid-19 is not the only airborne disease that we have suffered from. Besides the common cold and flu, Measles and Tuberculosis are other notorious airborne diseases that have taken many lives in the past decades and humans have experienced other pandemics like the Spanish flu in 1918 that was similar to Covid-19 [7,8]. So, it requires us to be ready to face the new probable pandemics.

There has been a great improvement in filter-based indoor air cleaning devices. HEPA filters are known to be capable of removing 99.97% of the airborne particles (including the infectious pathogens) thanks to various removal mechanisms that help the removal of particles of different sizes. Generally, inertial impaction is the mechanism by which larger particles are trapped while smaller particles stick to the fibres as a result of diffusion[9]. The problem with the HEPA filters though is that there is no mechanism for inactivation of the trapped particles and there is always a possibility of release of the attached particles back to the environment, especially close to the end of the lifetime of the filter when it is accumulated with particles and there is a likelihood of impaction of the new particles with the formerly trapped ones and also at the time of the filter change as the shake of the filter might cause detachment of the particles.

Usage of Ultra Violet type C (UVC) light has been proposed as a pathogen inactivation method since the short wavelength of irradiation in the range of $200 - 290nm$ is capable of corruption of the DNA/RNA of the pathogens and disables the virus replication capability[10]. However, the required exposure time for a satisfying pathogen load reduction (e.g. above 99%) is relatively high. Since the exposure time and the volumetric airflow rate have an inverse relation, it results in the restriction of the volumetric airflow rate to low numbers that

are insufficient for large-scale use. Consequently, although UVC has been widely used for sterilization of surfaces and objects where the exposure time is not a constraint [11], it does not seem to be an effective solution for air purification.

The use of heat is another method for inactivation of the pathogens which is widely studied for surface sterilization but they are restricted to relatively low temperatures, mostly below 100°C. [12]. On the other side, there are a handful of researches on thermal disinfection of the bulk air, and very few experimental studies are conducted on thermal inactivation of airborne diseases using high temperature.

Yap et al. [13] proposed a model to relate the exposure time and temperature. They knew that this correlation must be similar to the exponential correlations for other viruses and expected SARS-CoV-2 to also follow an alike first-order Arrhenius reaction equation and determined the unknown coefficients using the available experimental data.

Faucher et al. [14] simulated thermal inactivation of a facial mask at 90°C and estimated a 3-log reduction of the viral load according to the aforementioned Arrhenius equation. The air cooling process before inhalation of the sterilized air is not addressed in this work.

Jiang et al. [15] used mouse hepatitis virus (MHV), a beta coronavirus, in a solution that passes a 572μm diameter tube. The tube passes an oil bath, the temperature of which is adjustable. They tested two oil bath temperatures that resulted in the solution maximum temperature of 72 and 92°C. By adjusting the flow rate and subsequently the flow velocity, they were able to change the exposure time from 0.1 to 0.5s and obtained more than 5-log reduction.

Yu et al. [16] used a porous nickel foam as a filter to separate the pathogens from the contaminated air. They applied voltage to the metal foam to heat it to 200°C to kill the pathogens attached to the foam. They alleged a 99.8% efficiency for catch and kill of SARS-CoV-2 and a 99.9% efficiency for Bacillus anthracis. They reported that the air temperature increment was infinitesimal, meaning that all the escaped viruses are still infectious and only those that are trapped will be thermally inactivated. The thermal inactivation aspect of the project is not addressed in detail.

In this paper, we are aiming to both trap the particles and separate them from the contaminated air and also sterilize the air using a high-temperature inactivation method. For this purpose, multiple layers of fine woven nichrome mesh have been used that serve the purpose of both trapping the particles (potentially pathogens) similar to a regular fibrous filter and acting as a heating element to heat the airflow passing through it by applying a voltage to the mesh layers. Using ANSYS Fluent 2020, we numerically simulated the particle track and removal efficiency for different scenarios and calculated the bulk air temperature at the outlet of the domain.

II. METHODS

A. A brief review on the required temperature

According to Yap et al. [13], the required exposure time for achieving an n-log reduction of the virus load (t_{n-log}) at the exposed temperature T can be calculated based on the following equation:

$$t_{n-\log} = -\frac{1}{A} e^{\left(\frac{E_a}{RT}\right)} \ln(10^{-n}) \qquad (1)$$

Where A is the frequency factor, R is the gas constant, and E_a is the activation energy. They calculated E_a and A values for SARS-Cov-2 based on the available empirical data. To achieve a 3-log reduction, i.e. inactivation of 99.9% of the virus load, it requires $t_{3-\log}$ =2.38 minutes for T = 70°C, 3.12s for 100°C and 0.017s for 150°C. A short exposure time, $t_{n-\log}$, means the capability of sterilizing a large airflow rate. Therefore, taking the air temperature to 150°C is considered in the present work

B. Diagram of the apparatus

A general overview of the device is provided in Figure 1. The exhaust air which has passed the meshes and is both heated up and filtered enters a heat exchanger through which exchanges the excess heat with the pathogen-contaminated airflow before it passes through the mesh layers. It is beneficial in two ways: first, the hot exhaust airflow will lose a considerable fraction of the excess heat and depending on the desired discharge temperature, can be released back to the environment or be directed to an extra cooling process before the discharge. Furthermore, the inlet airflow will preheat before passing through the meshes. Depending on the heat exchanger efficiency, this process can save up to 90% of the consumed energy in the mesh heating elements.

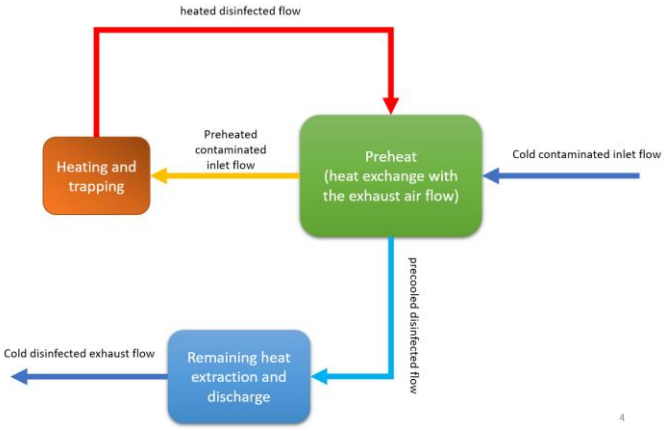

Fig.1: Overview diagram of the apparatus

C. Geometry and mesh

Eight layers of fine woven nichrome mesh are placed consecutively at a specified distance. As illustrated in Figure 2, Each wire diameter, D_w, is 100 μm and the hole size, H, (the distance between two wires in a single layer) is 200μm. Different distances of $D = 200, 300, 500\mu m$ between two consecutive mesh layers have been studied. The mesh layers

serve both as heating elements to heat the airflow up to the desired $150°C$ temperature and also as a filter to capture the particles. In order to increase the coverage of the mesh wires in the space and therefore increase the probability of the capture of the particles, each mesh layer is rotated at a random angle around the axis parallel to the airflow direction.

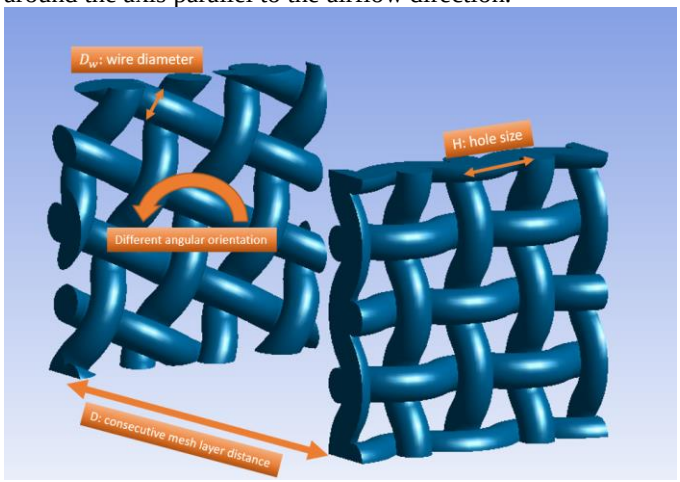

Fig.2: an image of the fluid domain with the mesh layers subtracted

The real-size device is designed to be a duct with a $25 \times 25\ cm$ cross-section in which the mesh layers are implemented and can provide a $5\frac{m^3}{min}$ flow rate. A duct with a cross-section of $0.8 \times 0.8\ mm$ is considered as a small portion of the whole fluid domain for the numerical simulation. The symmetry boundary condition is applied to all the sidewalls of the duct and the proper wall heat flux is contributed to the surfaces where mesh layers come in contact with the air zone, to achieve 150°C outlet temperature.

A total number of 16.8 million tetrahedron mesh elements (for the case with $200\mu m$ distance between the layers) are generated using ANSYS Meshing software.

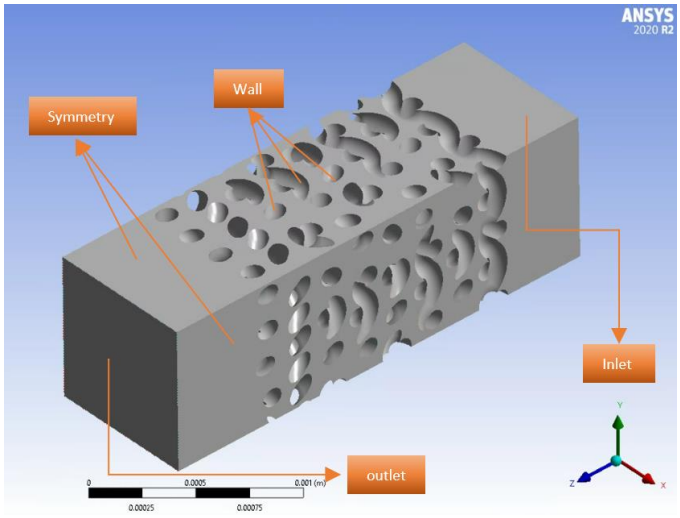

Fig.3: An image of the fluid domain as the wall mesh layers are subtracted from duct block along the boundary conditions.

D. Software setups

The fluid domain is solved by Eulerian equations and the Lagrangian method was used to track the particles. $SST\ K-\omega$ turbulence model was used to simulate the airflow and the particle trajectories were calculated using the Discrete Phase Model (DPM) implemented in ANSYS Fluent. Monodisperse parcels were injected from the center of each cell at the inlet of the domain at the airflow inlet velocity and temperature. Inert particles have the same properties as liquid water. According to the target $5\frac{m^3}{min}$ flow rate in the real-size device, inlet mass flow rate was set proportionate to the simulation geometry scale-down size (i.e. $\frac{0.8\ mm}{25\ cm}$). The DPM boundary condition for the walls was set to trap (i.e. particles will be counted as trapped and removed from the domain as soon as they come in contact with any of the mesh walls). The symmetry boundary condition is applied to all the sidewalls of the duct since the simulation geometry is a small fraction of the $25 \times 25\ cm$ real-size duct. Uniform surface heat flux is applied to all the wire surfaces which are in contact with the airflow.

Both the continuous and discrete phases were solved in a steady-state condition and the one-way interaction status was set since the mass density of the particles was infinitesimal as opposed to the fluid. (i.e. only fluid influences on the particle track, and not vice versa)

III. RESULTS AND DISCUSSION

A. Validation of the Lumped capacity method

In the Discrete Phase Model (DPM), the heat transfer for each particle is based on lumped capacitance method. Here we will check the validity of this method for this work by evaluating the Biot number.

The uniform temperature assumption for a substance is valid if the Biot number is small i.e. $Bi \ll 1$. Biot number is defined as $Bi = \frac{hD_p}{2k}$ where h, D_p, k are convective heat transfer coefficient, particle diameter and particle thermal conductivity respectively [17]. This is an important issue to assure that the nucleus of the particle has the same temperature as the surface since most of the virus particles are assumed to be in the nucleus of the droplet (which is at the center of the droplet).

h can be evaluated based on the average Nusselt number of the particles along their path from the inlet to the outlet of the duct that can be reported from Ansys Fluent.

$$Nu = \frac{hD}{k} \qquad (2)$$

Where D and K are the particle diameter and air thermal conductivity respectively. All the fluid properties are calculated at mean temperature ($T_m = \frac{T_i+T_o}{2} = \frac{25°C+150°C}{2} = 87.5°C$)

According to the particle track results, for $1\ \mu m$ particles as a sample size, the particles Nu number range is [2,2.4]. So, the average Nu number is 2.2. Subsequently, $h = 67650\frac{j}{kg.k}$.

Considering $D_p = 1\ \mu m$ and the fact that the droplet is fully composed of water, Biot number was reported to be $Bi = 0.05$ at the outlet of the domain for the escaped particles (i.e. not trapped at the walls). Consequently, it is a solid conclusion that the particle temperature is uniform throughout the sphere.
According to the definition, the Biot number has a direct relationship with the diameter of the particle, so Bi will be even smaller for smaller particles. Hence, the particle temperature can be assumed uniform.
Now that a spatially uniform temperature in the droplet spheres is a reasonable assumption, the thermal time constant (τ) can be calculated based on the Lumped Capacitance Method.

$$\tau = \left(\frac{1}{hA_s}\right)(\rho V c_p) \qquad (3)$$

Where A_s, ρ, V *and* c_p are the spherical surface area of the droplet, air density, sphere volume and droplet heat capacity respectively [17]. τ is the required time for the particle to reach the same temperature as the flow's.
Substitution of the relevant parameters results in $\tau = 2.44 \times 10^{-9}\ s$. On the other side, the average flow velocity is $U = 1.568 \frac{m}{s}$ according to Fluent report. Here a dimensionless parameter is defined to compare the thermal time constant to the average particle travel time in the duct.

$$\gamma = \frac{\tau U}{D} \qquad (4)$$

Where D is the distance between two consecutive mesh layers. Our worst scenario is the $D = 500\mu m$ geometry. Substitutions result in $\gamma = 7.65 \times 10^{-6}$ which is insignificant. It means that the required time for the particle temperature to be affected by the airflow is substantially smaller than the average time that takes a particle to travel between two mesh layers, where the next temperature raise step happens. Accordingly, it can be concluded that the particles have the same temperature as the flow almost instantaneously.

B. *Impact of the particle size on the particle removal*

Particle removal efficiency is defined as the fraction of the number of trapped particles at the wires to the total number of injected particles. A diagram of the particle removal efficiency based on the particle size is provided in figure 3. Particle removal efficiency is predicted using the Stokes parameter which is defined as the ratio of the distance a particle travels before it comes to stop, to a characteristic length.

$$Stk = \frac{\rho_p D_p^2 U_0}{18 \mu D_w} \qquad (4)$$

Where ρ_p *and* D_p are particle density and diameter, U_0 and μ are air velocity and dynamic viscosity, and D_w is the wire diameter in this study.

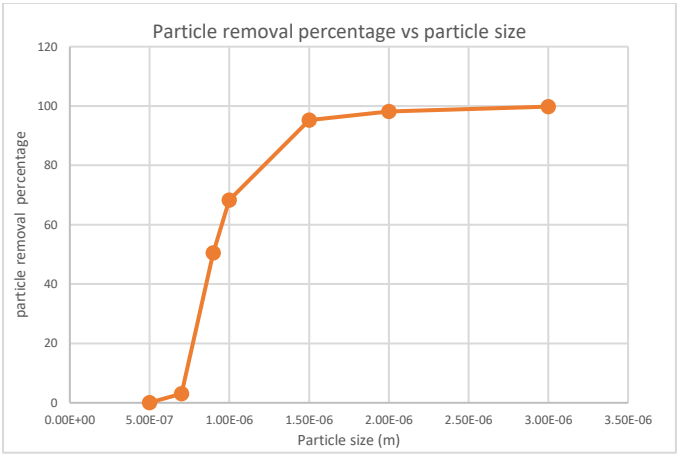

Fig.4: Particle removal efficiency for different particle sizes

Larger particles have greater momentum and it is harder for them to follow the sharp pathline changes so they get trapped at higher rates. As the particle size decreases, it is less likely that they hit the wire meshes since the corresponding Stokes number is smaller for them and they can move along the airflow. Most of the particle traps occur by the first two mesh layers for the $3\mu m$ particles while the first mesh layer does not trap any $1\mu m$ particles. In the latter case, The first layer mainly acts as a turbulence intensifier which disturbs the flow. While particles can pass the first layer due to low Stokes number, the next layers are located at a small distance in a way that the particles won't have sufficient time to surpass them and will hit them. Particles smaller than $1\ \mu m$ have such low Stokes number that can follow the airflow easily without hitting the wires and getting trapped. According to figure 3, $D_{50} = 0.9\ \mu m$ which indicates that 50%- removal efficiency happens for $0.9\ \mu m$ particles in this device.

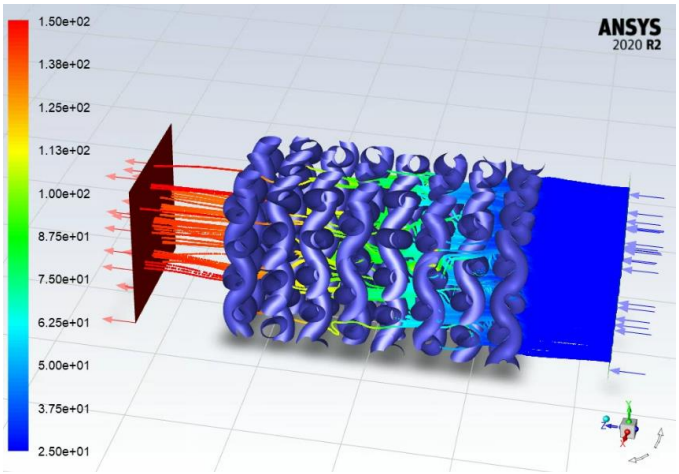

Fig.5: $1.5\mu m$ Particle tracks, coloured by particle temperature

Particle paths are tracked and illustrated for $1.5\mu m$ particles. The particles are point-injected at various spots at the inlet and gradually get trapped by the wire surfaces and heat up along their path toward the outlet. It was noticed in other simulations that the overall particle removal decreases as the gap between the mesh layers increases.

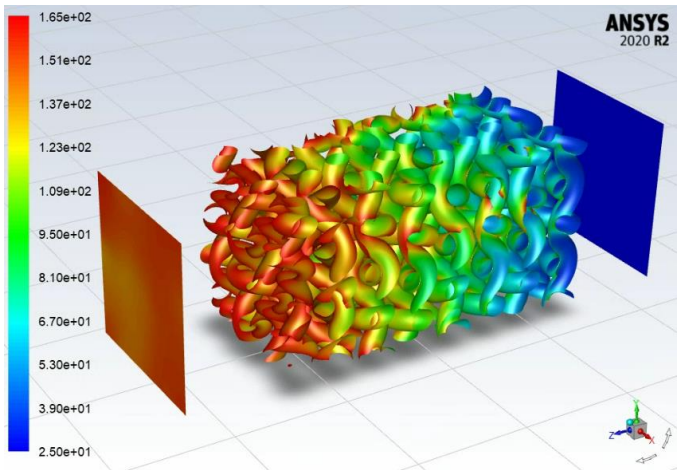

Fig.6: 1.5μm Particle tracks, coloured by particle temperature

Wall temperatures accompanying the inlet and the outlet temperature contours are depicted in Figure 5. The last wall reaches the maximum temperature of $160°C$.

II. CONCLUSION

In this study, a numerical simulation is carried out using ANSYS Fluent to evaluate the thermal performance and particle removal efficiency of a novel concept. Pathogen-contaminated airflow passes through multiple layers of finely woven nichrome meshes that both trap the particles and heat the air up to 150°C. This is the required temperature for the 3-log virus load reduction at 0.017s exposure time, according to the exponential relationship of the temperature and the exposure time models. It was proved that the particles will have the same temperature as the flow and $D_{50} = 0.9\ \mu m$ which means that 50%-removal efficiency occurs for $0.9\ \mu m$ particles in this device. The energy consumption can be reduced significantly using a heat exchanger to transfer the excess heat from the exhaust flow to the intake airflow and preheat it. Experimental tests are in progress to validate the numerical data.

REFERENCES

[1] WHO, "WHO Coronavirus (COVID-19) Dashboard," *World Health Organisation*, 2021. https://covid19.who.int/.

[2] G. Jiang *et al.*, "Aerosol transmission, an indispensable route of COVID-19 spread: case study of a department-store cluster," *Front. Environ. Sci. Eng.*, vol. 15, no. 3, 2021, doi: 10.1007/s11783-021-1386-6.

[3] X. Zhang, Z. Ji, Y. Yue, H. Liu, and J. Wang, "Infection Risk Assessment of COVID-19 through Aerosol Transmission: A Case Study of South China Seafood Market," *Environ. Sci. Technol.*, vol. 55, no. 7, pp. 4123–4133, 2021, doi: 10.1021/acs.est.0c02895.

[4] R. Zhang, Y. Li, A. L. Zhang, Y. Wang, and M. J. Molina, "Identifying Airborne Transmission as the Dominant Route for the Spread of COVID-19," *COVID-19 Read.*, pp. 21–35, 2020, doi: 10.4324/9781003141402-3.

[5] "Science Brief: COVID-19 Vaccines and Vaccination," 1375. https://www.cdc.gov/coronavirus/2019-ncov/science/science-briefs/fully-vaccinated-people.html.

[6] C. Smith-Schoenwalder, "A Fourth Coronavirus Shot Will Likely Be Needed. But Questions Remain About When and What Kind." https://www.usnews.com/news/health-news/articles/2022-01-13/a-fourth-coronavirus-shot-will-likely-be-needed-but-questions-remain-about-when-and-what-kind.

[7] S. Basco, J. Domenech, and J. Rosés, "The Redistributive Effects of Pandemics: Evidence on the Spanish Flu," *Ssrn*, 2020.

[8] T. Kertscher, "Fact-check: Has a pandemic occurred every 100 years?," *Statesman*, 2020. https://www.statesman.com/news/20200410/fact-check-has-pandemic-occurred-every-100-years.

[9] G. Berry, A. Parsons, M. Morgan, J. Rickert, and H. Cho, "A review of methods to reduce the probability of the airborne spread of COVID-19 in ventilation systems and enclosed spaces," *Environ. Res.*, vol. 203, 2022, doi: 10.1016/j.envres.2021.111765.

[10] S. K. Bhardwaj *et al.*, "UVC-based photoinactivation as an efficient tool to control the transmission of coronaviruses," *Sci. Total Environ.*, vol. 792, 2021, doi: 10.1016/j.scitotenv.2021.148548.

[11] Z. Michelini *et al.*, "Ultraviolet sanitizing system for sterilization of ambulances fleets and for real-time monitoring of their sterilization level," *Int. J. Environ. Res. Public Health*, vol. 19, no. 1, 2022, doi: 10.3390/ijerph19010331.

[12] J. P. Abraham, B. D. Plourde, and L. Cheng, "Using heat to kill SARS-CoV-2," *Rev. Med. Virol.*, vol. 30, no. 5, 2020, doi: 10.1002/rmv.2115.

[13] T. F. Yap, Z. Liu, R. A. Shveda, and D. J. Preston, "A Predictive Model of the Temperature-Dependent Inactivation of Coronaviruses," *ChemRxiv*, 2020, doi: 10.26434/chemrxiv.12152970.

[14] S. Faucher *et al.*, "A virucidal face mask based on the reverse-flow reactor concept for thermal inactivation of SARS-CoV-2," *AIChE J.*, vol. 67, no. 6, 2021, doi: 10.1002/aic.17250.

[15] Y. Jiang *et al.*, "Sub-second heat inactivation of coronavirus using a betacoronavirus model," *Biotechnol. Bioeng.*, vol. 118, no. 5, pp. 2067–2075, 2021, doi: 10.1002/bit.27720.

[16] L. Yu *et al.*, "Catching and killing of airborne SARS-CoV-2 to control spread of COVID-19 by a heated air disinfection system," *Mater. Today Phys.*, vol. 15, 2020, doi: 10.1016/j.mtphys.2020.100249.

[17] F. P. Incropera and D. P. DeWitt, *Fundamentals of Heat and Mass Transfer*. 1996.